Heliyon 6 (2020) e05784

Contents lists available at ScienceDirect

Heliyon

journal homepage: www.cell.com/heliyon

Research article

Electrodeposition of silver onto carbon graphite and their catalysis properties toward thiamethoxam reduction: application in food and beverage samples

N. Ajermoun [a], S. Lahrich [a], A. Farahi [a], M. Bakasse [b], S. Saqrane [a], M.A. El Mhammedi [a,*]

[a] Sultan Moulay Slimane University, Laboratory of Chemistry, Modeling and Environmental Sciences, Polydisciplinary Faculty, Khouribga, Morocco
[b] Chouaib Doukkali University, Organic Micropollutants Analysis Team, Faculty of Sciences, Morocco

ARTICLE INFO

Keywords:
Thiamethoxam
Silver particles
Electrodeposition
Graphite carbon electrode

ABSTRACT

The purpose of this paper is the electrodeposition of silver particles on graphite electrode (Ag@GrCE) using chronoamperometry and the use of this electrode for the determination of thiamethoxam. The electrode was prepared by chronoamperometry and characterized by X-Ray diffraction (XRD), fourier transform infrared spectroscopy (FT-IR), EDX analysis and electrochemical impedance spectroscopy. The obtained electrode exhibits excellent electrocatalytic activity toward thiamethoxam reduction. The voltammetric response was linear as function of TXM concentration with a limit of detection around to 1.92×10^{-6} mol L^{-1}. The proposed electrode was successfully used to analyze thiamethoxam residue in some food samples including orange and tomato juices.

1. Introduction

Neonicotinoid insecticides are a new generation of pesticides introduced onto the market since 1980s [1] as a principal alternative for pesticides [2] after domination of organophosphate and carbamate in the world pesticides market [3, 4]. Based on their good effectiveness and low toxicity toward mammals and environment [1, 2, 5, 6, 7, 8], neonicotinoids insecticides are a type of pesticides that act on the nicotinic acetylcholine receptor (nAChRs) in the central nervous system of insects, causing paralysis and death. They are systemic and environmentally persistent: they can be existing in the nectar, pollen, and guttation droplets that bees collect [9, 10]. The class of neonicotinoids was synthesized from of the chloropyridine compounds [11, 12], first one among these, generated with a chlorothiazole heterocycle in place of the chloropyridine named thiamethoxam (3-[(2 chloro-5-thiazolyl)methyl] tetrahydro-5-methyl-N-nitro-4H-1,3,5-oxadiazin-4-imine) [13, 14] that is a second generation neonicotinoid widely used [15] for pest control in foliar, soil and seed treatment [16, 17]. Due to its persistence, low soil adsorption, low biodegradability, high leaching capacity, and high solubility in water [18], thiamethoxam has become a potential pollutant in surface water and groundwater, which could pose a serious threat to aquatic organisms and public health. Therefore, it is necessary to develop sensitive techniques to detect thiamethoxam at trace levels. Hitherto, various analytical methods have been developed to determine the thiamethoxam in different samples. The chromatographic techniques, such as High-Performance Liquid Chromatography (HPLC), HPLC-Mass Spectrometry-Mass Spectrometry (HPLC-MSMS) or Gas Chromatographic-MSMS (GC-MSMS) [19, 20, 21, 22], in addition to Enzyme-Linked Immunosorbent Assay (ELISA) [23, 24, 25], have been developed to determine the neonicotinoids insecticide. Also, the TXM analysis was performed by electrochemical methods where several materials [5, 7, 8, 26, 27, 28, 29, 30, 31] have been used as working electrodes. In recent years, they are appeared as alternatives for pesticides detection, with benefits related to the low cost, simplicity, high sensitivity and waste reduction, among others. Modification of the surfaces of such sensors with particle, nanoparticles can enhance these advantages. In electroanalysis, carbon-based materials e.g. glassy carbon, graphite, diamond and sol-gel have been extensively employed, due to their high conductivity, wide potential window and low background response [32, 33, 34, 35]. The silver particles could not only improve the sensitivity of detection for some organic compounds, but also could be applied to the catalysis of their electrochemical reaction [36]. The electrochemical reduction of thiamethoxam based on reduction of its nitro group via four electron process to generate the hydroxylamine derivative [37, 38, 39, 40]. In this context, we proposed here a novel electrochemical approach for TXM analysis that based on the electrodeposition of silver particles on graphite electrode (Ag@GrCE) using chronoamperometry. The Ag@GrCE was used for to the electro-reduction of TXM in

* Corresponding author.
E-mail address: elmhammedi@yahoo.fr (M.A. El Mhammedi).

https://doi.org/10.1016/j.heliyon.2020.e05784
Received 26 August 2020; Received in revised form 18 October 2020; Accepted 16 December 2020

britton-robinson (B-R) buffer (pH 10.4). The catalytic parameters such as: electro-active surface coverage (Γ), the transfer coefficient, (α), the catalytic rate constant and the diffusion coefficient (D) were calculated. The transport processes and reaction mechanism involved in the reduction reaction of thiamethoxam at Ag@GrCE were determined. Finally, the prepared electrode was used to determine thiamethoxam in tomato and orange simples using square wave voltammetry.

2. Experimental

2.1. Chemicals and reagents

Concentration of 8.0×10^{-4} mol L^{-1} of $AgNO_3$ (p.a 98% sigma Aldrich) in britton-robinson buffer pH 2.0 was used for the electrodeposition of silver on graphite electrode. The stock solutions were prepared from analytical reagents and distilled water. Acetic acid, phosphoric acid, boric acid and sodium hydroxide were obtained from Merck (Darmstadt, Germany), Fluka (st. gallen, Switzerland), Riedel de Haen (seelze, Germany). The thiamethoxam pesticide (commercial formulation Actara 25-WG (250 g k^{-1}) obtained from Syngenta international AG (Basel, Switzerland) was dissolved in Britton-Robinson buffer (pH 10.4) to prepare stock solution of 1.0×10^{-2} mol L^{-1} thiamethoxam and stored in dark. Graphite was provided from carbon Lorraine (Lorraine, France ref 9900).

2.2. Instruments and methods

Electrochemical measurements were carried out by Voltalab potentiostat (model PGZ 100; Eco Chemie B.V, Utrecht, The Netherlands) operated by voltamaster 4 software as an electrochemical system data processing software, in conventional three electrodes connection including: silver modified graphite carbon (Ag@GrCE) as working electrode, Ag/AgCl/3M KCl reference electrode and platinum wire counter electrode. The pH meter (Radiometer, SENSION, pH 3, Leganes Spain) was employed for adjusting pH values. SEM observations were carried out using the JOEL JSM-IT100 scanning electron microscopy. Powder X-ray diffraction (XRD) patterns were recorded on an XRD (D2 PHASER of BRUKER-AXS) with X-ray source emitting Cu Kα radiation (k = 1.5406 Å) and scans acquisition at 2θ range from 10° to 80°, as can speed of 1°/min and step size of 0.02° per second. Fourier transform infrared (FT-IR) spectra of Ag@GrC were performed in the frequency range of 400–4000 cm^{-1} by VORTEX 70 DTGS spectrometer using KBr pallet method.

2.3. Electrodeposition and analysis procedure

The chronoamperometry was employed for the electrodeposition of silver particles modified graphite carbon electrode, in the electrolyte (volume 25 mL) of britton-robinson pH 2.0 containing 8.0×10^{-4} mol L^{-1} of silver nitrate. For this procedure, we use an electrode cavity (0.13 cm^2) and a graphite bar to finding the electrical contact. The prepared electrode carefully washed by distilled water and transferred into a cell (25 mL volume) containing thiamethoxam in britton-robinson pH 10.4. The square wave voltammetry was reported in the range from -400 mV to -1400 mV.

2.4. Preparation of real samples

The fruits tomato and orange were purchased from the local market of khouribga, morocco. The tomato and orange were cleaned using distilled water, and blended employing a blender. Then, in order to have a juice solution without pulps and more clear, the residue undergoes several filtrations on filter paper. To adjust the pH value of juice, the britton-robinson buffers have been added to samples. Finally, the juice spiked by adding an appropriate amount of TXM, and transferred to an electrochemical cell. The square wave voltammetry was used to TXM analysis.

3. Results and discussion

3.1. Electrodeposition process of Ag and its efficiency for TXM sensing

Electrochemistry is a science of surfaces and interfaces that studies the chemical reactions that take place at the electrode-electrolyte interface. Electrodes are the main constituents in all electrochemical applications. The ability to modify their surface structure allows electrochemical systems to evolve. Electrodeposition is simple, controllable, low-cost and time-saving technique in comparison with other methods, such as physical and chemical vapour deposition, hydrogen plasma, hydrothermal and sonochemical methods. Also offer the advantage of being able to assembling nanostructured multi-component films. Various features of silver electrodeposition on electrode surface to control the composition and morphology of incorporated particles in the coatings were reported for electroanalytical applications, such as organic compound and heavy metal analysis, via different manufacture and flexibly design of silver electrodeposited. Majidi et *al.* introduced a novel electrochemical sensor based on AgNDs supported by graphene nanosheets modified GCE for imidacloprid determination [41]. Laghrib et *al.* determined para-nitroaniline and studied its electrocatalytic reduction using silver particles electrodeposited onto carbon-paste electrodes by cyclic voltammetry [40, 42]. An electrodeposition of silver amalgam particles (AgAPs) on basal-plane pyrolytic graphite electrode (bPGE), and prove on 4-nitrophenol [43]. Feng-Hsuan Cho et *al.* prepared silver dendrites (Ag-Ds) by electrodeposition on a glassy carbon electrode (GCE) and investigated its capability in sensing 4-nitrophenol, via surface enhanced raman scattering (SERS) using laser excitation at 633 nm [44]. Jia Bi has developed an electrodeposition approach to provide silver nanoflowers composed of many silver nanoleaves as sensitive surface enhanced raman scattering sensing substrates [45]. In the same context, the results present by Joaquín Klug et *al.* showed direct interaction between the Myristoylated Alanine-Rich C Kinase Substrate (MARCKS) effector domain (ED) and Ag nanoparticles (AgNPs) electrochemically deposited on the silicon platform as surface enhanced raman scattering substrate [46]. Also, Mehdi Baghayeri and co-work adopted an electrochemically deposition of silver nanoparticles on the film of a metformin functionalized multi-walled carbon nanotube modified glassy carbon electrode (Met-MWCNT/GCE) for entacapone (ENT) determination [47]. Simultaneous electrochemical sensing of chloramphenicol and metronidazole are investigated by Haiyun Zhai et *al.* using electrodeposited silver nanoparticles/sulfonated functionalized graphene modified glassy carbon electrode (AgNPs/SF-GR/GCE) [48]. The same method was reported by Lorena Athie Goulart et *al.* for analysis of four phenolic compounds using a glassy carbon electrode (GCE) modified with electrodeposited silver nanoparticles onto multi-walled carbon nanotubes [49]. A glassy carbon electrode (GCE) modified by electrodeposited silver nanoparticles AgNPs as an electrochemical nanoaptasensor was used to determine trinitrotoluene [50]. Mercury ions were detected by silver nanoparticles as signal reporter selectively electrodeposited on glassy carbon electrode modified with DNA-based AuHg amalgam [51]. All these modifications were done in order to enhance the electrode sensitivity and others lead to high electrocatalytic activity. Tiwari et *al.* have investigated an electrodeposition technique, which provided a suitable route for the synthesis of silver coated nitrogen rich mesoporous carbon (Ag/NMC) composite for the electrocatalytic activity towards ORR (oxygen reduction reaction) [52]. Agnieszka Brzózka and co-works reported the elecrodeposition of silver nanohemisphere (Ag–NHS) and nanowire (Ag-NW) array into nanoporous aluminum oxide (AAO) templates where they compared their electrocatalytic properties against silver rod (Ag-bulk) electrode in an alkaline solution [53]. In our study, due to high importance of electrochemical deposition process, the chronoamperometry was employed

to deposit silver particles onto graphite carbon. This modified electrode was used for the TMX determination.

The electrocatalytic capacity of the Ag@GrCE toward electrocatalysis of thiamethoxam (TXM) reduction was evaluated by cyclic voltammetry (CV) and square wave voltammetry (SWV). The cyclic voltammograms show a cathodic peak at -1186 mV and -1083 mV on graphite carbon electrode (GrCE) and graphite carbon modified electrodeposited silver particles electrode (Ag@GrCE) respectively (Figure 1a). Under identical conditions, square wave voltammetry (SWV) confirms the same behaviour of Ag@GrCE toward reduction of TXM. In fact, a reduction peak is observed at -1186 mV and -1083 mV on GrCE and Ag@GrCE respectively (Figure 1b). Therefore, the Ag@GrCE presents great enhanced current response of the reduction peak, which due to the enhanced in surface conductivity with the presence of silver particles. Moreover, the peak potential shifted ~100 mV positively in the TXM reduction potential, which due to the electrocatalytic activity of silver particles [54].

3.2. Optimization of electrodeposition conditions

For deposit of the silver particles onto carbon with catalytic properties, it is essential to optimize the parameters influencing the detection of thiamethoxam by the SWV (deposition time, concentration of silver in electrolyte, solution pH and applying potential …). The effect of the deposition time of silver particles on the SWV response of TXM was investigated in a solution of B-R buffer (pH 10.4) containing 1.0×10^{-3} mol L^{-1} of TXM in the potential range from -0.4 to -1.4V. The maximum peak current was obtained with 4 min (Figure 2a), more this time, the peak current values decrease. The applying potential is an important parameter in chronoamperometric measurements. For the right choice of this potential, several potentials were tested (Figure 2b) to have a good electrodeposition of silver particles on graphite surface. The Ag@GrCE electrode prepared at applied potential of -400 mV shows higher sensitivity toward TXM sensing. The amount of silver on the electrode surface is also necessary to assess the electrochemical determination of thiamethoxam. Therefore, it was optimized by varying the concentration of $AgNO_3$ in range from 1.0×10^{-4} to 1.0×10^{-3} mol L^{-1} of $AgNO_3$ in B-R buffer pH 2.0 with the evaluation of its effect on response of TXM. Under optimized parameters, applying potential of -400 mV for 4 min, the 8.0×10^{-4} mol L^{-1} of $AgNO_3$ shows the highest peak intensity. However, high concentration of $AgNO_3$ shows low response of TXM (Figure 2c). This behaviour was attributed to the formation of a large number of small clusters randomly distributed on the GrC electrode surface [36]. The electrodeposition parameters were as follows: 4 min, 8.0×10^{-4} mol L^{-1}, pH 2.0 and -400 mV for deposition time, concentration of silver in electrolyte, solution pH and applying potential, respectively.

3.3. Surface characterization of Ag@GrCE

The surface morphology of the Ag@GrCE was investigated by scanning electronic microscope (SEM). The image revealed that carbon had two dimensional flat morphology exhibits a homogeneous and compact layer with small particles and full coverage (Figure 3a). To confirm the presence of the silver particles, the EDS was used. In EDS analysis, Figure 3b shows the peaks in silver region confirming the presence of elemental silver [55]. To confirm this result, XRD pattern silver/graphite were obtained as illustrate in Figure 3c. The four diffraction peaks are observed at 2θ of 38.15, 44.19, 64.41 and 77.32, which can be designated respectively to diffraction from the planes (111), (200), (220) and (311) of the face centred structure of Ag(0), (JCPD, file No. 4-0183) [56].

The electroactive surface area (ESA) has been estimated using cyclic voltammetry of solution containing 1.0×10^{-2} mol L^{-1} of $[Fe(CN)_6]^{3-/4-}$ containing 0.1 mol L^{-1} KCl at different scan rates (ν) ranging from 0.005 V s^{-1} to 0.3 V s^{-1} according to Randles-Sevcik Eq. (1).

$$Ip = 2.69\times10^{5}\times n^{3/2}\times A\times D^{1/2}\times C\times\nu^{1/2} \quad (1)$$

Both the peak currents (Ip) of the GrCE and Ag@GrCE were proportional to the square root of scan rate (Figure 4a-b). Considering $D = 7.6\ 10^{-6}$ cm^2 s^{-1} and $n = 1$ for a 1.0×10^{-2} mol L^{-1} of $[Fe(CN)_6]^{3-/4-}$ and from the slopes values of the straight lines. The ESA of GrCE and Ag@GrCE were obtained are 1.08×10^{-4} cm^2 and 2.25×10^{-4} cm^2 respectively. The electroactive surface area of Ag@GrCE increased approximately by 48.04% compared to the GrCE, demonstrating the enhancing conductivity of modified electrode.

To calculate the heterogeneous electron transfer (ET) rate k°, the Nicholson method was used from the peak-to-peak separation ΔEp of the cyclic voltammogram. As shown in Figure 4a-b, the ΔEp is increased with scan rate, indicating a quasi-reversible nature of reaction, using following Eq. (2) [57].

$$\Psi = k^{\circ}[\pi n D\nu F / RT]^{-1/2} \quad (2)$$

Where ψ is the dimensionless kinetic parameter, n is number of electrons transferred, D is the diffusion coefficient, F faradic constant, R the gas constant, T the temperature of solution and ν the scan rate. In practice, the kinetic parameter ψ is calculated from ΔEp for one step, one electron process at a set temperature 298 k, using an appropriate practical function (equation 3) [58].

$$\Psi = (-0.628 + 0.021\Delta Ep) / (1–0.0071\Delta Ep) \quad (3)$$

The heterogeneous electron transfer (ET) rate constant k° was determined from the slope of ψ-$[\pi nDF/RT]^{-1/2}$ $\nu^{-0.5}$ dependence corresponding to Eq. (2) as shown in Figure 4a-b, while the operating curve

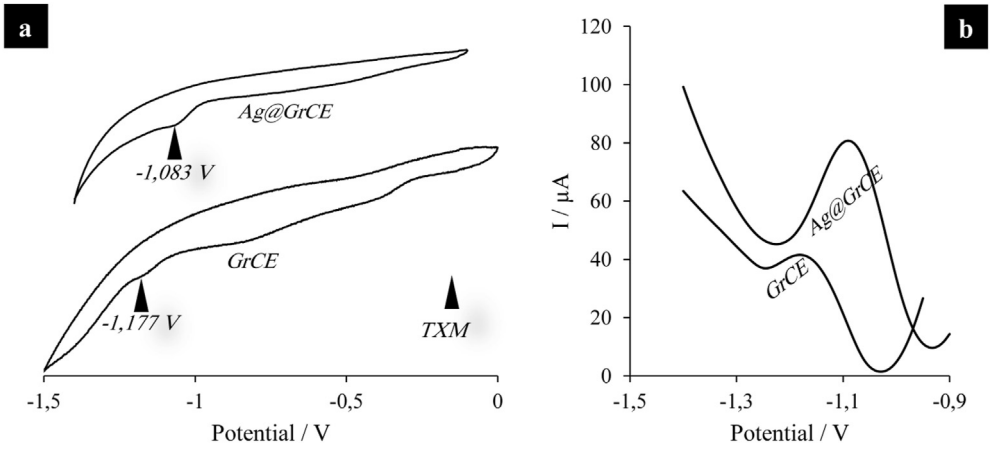

Figure 1. (a) Cyclic voltammetric response, (b) square wave voltammetric response of 1.0×10^{-3} mol L^{-1} thiamethoxam respectively at electrodeposited silver particles on graphite carbon electrode (Ag@GrCE) and graphite carbon electrode (GrCE) in R–B buffer pH 10.4.

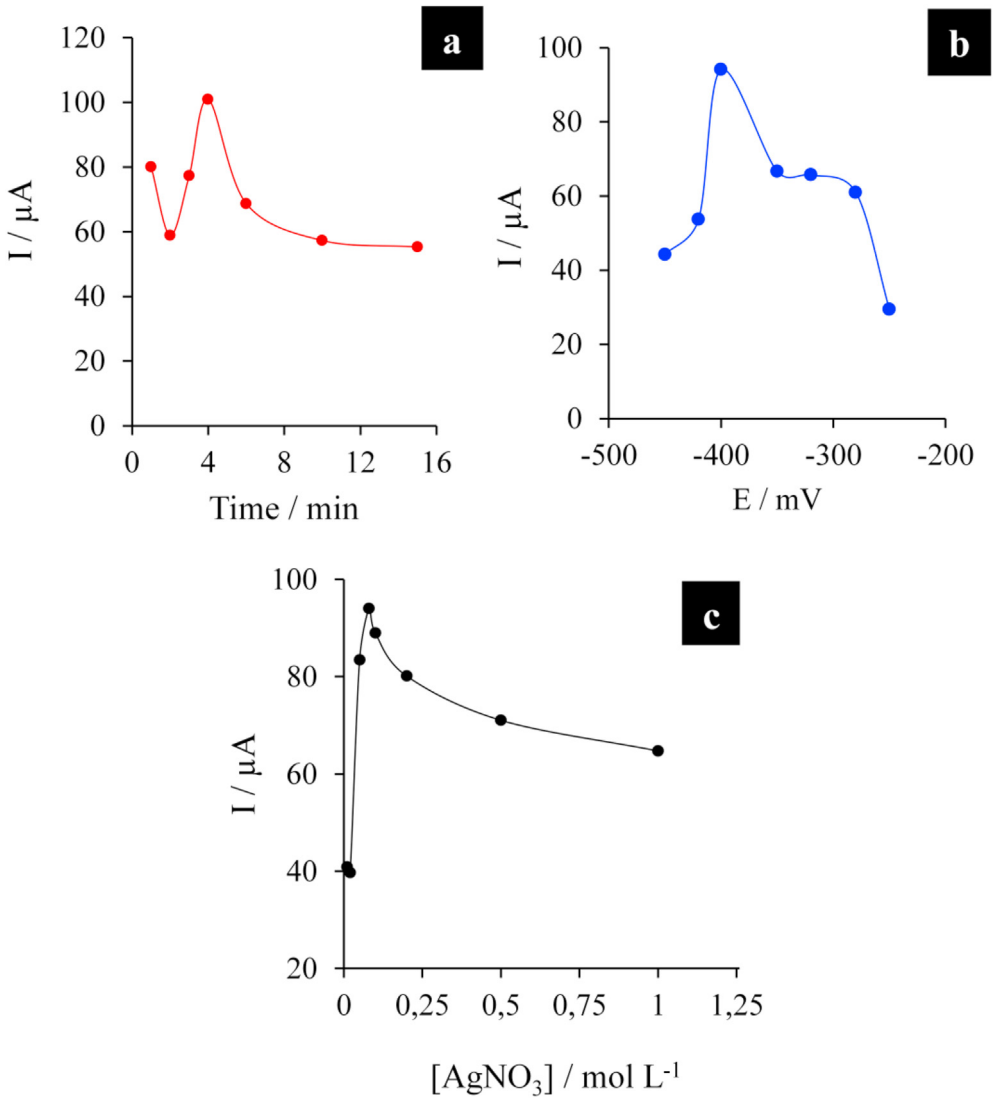

Figure 2. Influence of the experimental parameters, on chrononoamperometric electrodeposition: (a) the electrodeposition time, (b) the applying potential and (c) the amount of $AgNO_3$ on the reduction peak current of 1.0 × 10^{-3} mol L^{-1} TXM. Square wave voltammograms measurements were performed in B-R buffer (pH 10.4).

determined according to this approach is limited to ΔEp occurred in the interval ˃ 212 mV. A method devised by Kochi and Klinger permits the use of much large ΔEp for k° evaluation following Eq. (4) [59].

$$K^{\circ} = 2.18[D\alpha n\nu / RT]^{-1/2}Exp[-(\alpha^2 Nf / RT)\,\Delta Ep] \quad (4)$$

The ET rate k° was calculated to correspond to 8.84 × 10^{-4} cm s^{-1} and 1.09 × 10^{-3} cm s^{-1} for both electrode GrCE and Ag@GrCE respectively using the above equations. The results suggesting that the electron transfer reaction were easily transferred on the surface modified silver particles.

For explain the effect of electrodeposition potential onto formation of the silver particles, the surface properties of the different electrodes prepared were investigated using electrochemical impedance spectroscopy (EIS). Also, to evaluate the electron-transfer kinetic of the modified electrode by silver particles, solution of 0.1 mol L^{-1} KCl containing 1.0 × 10^{-2} mol L^{-1} of $[Fe(CN)_6]^{3-/4-}$ was used. The nyquist diagrams of Ag@GrCE prepared at different applied potentials (-300 mV, -400 mV and -500 mV) and GrCE were recorded in the range of 100 Hz to 100 MHz (Figure 4c). Indeed, the dielectric and insulating properties of the electrode/electrolyte interface depend on the charge transfer resistance R_{ct}, which corresponds to the diameter of the semicircle observed at high frequencies in Nyquist diagrams. All Ag@GrCE showed a higher electron transfer kinetic compared of unmodified electrode prepared GrCE (Figure 4c). The R_{ct} of the Ag@GrCE (-400 mV) was measured to be (72.09 Ω cm^2), which is lower than Ag@GrCE (-300 mV; 120.3 Ω cm^2) and Ag@GrCE (-500 mV; 89.31 Ω cm^2). The Ag@GrCE (-400 mV) presented an excellent electronic property, forming a fast electron conduction pathway between the electrode and the electrochemical probe when compared with others electrodes.

Following EIS characterization and to investigate the functional groups of modified graphite, FT-IR measurements were recorded at the range 4000–400 cm^{-1}. The spectra obtained for silver particles electrodeposited on graphite electrode applying various deposition potentials (-300, -400 and -500 mV) are given in Figure 5. A broad band at 3444 cm^{-1} is attributed to the –O-H group into the external surface of graphite carbon. The two bands at 2921 and 2855 cm^{-1} in the higher frequency region of spectra correspond to C–H stretching mode, while the two shoulder peaks at 1632 and 1580 cm^{-1} can be ascribed to aromatic C=C and C–C or C–O groups, which exists on a sample of silver-graphite carbon (Ag@GrC) surface as functional groups prepared applying a potential of -500 mV.

The spectra of the Ag@GrC samples prepared applying -400 and -300 mV obtained are similar to that Ag@GrC prepared at -500mv surface, with the exception that all the bands shift to low wave numbers, which

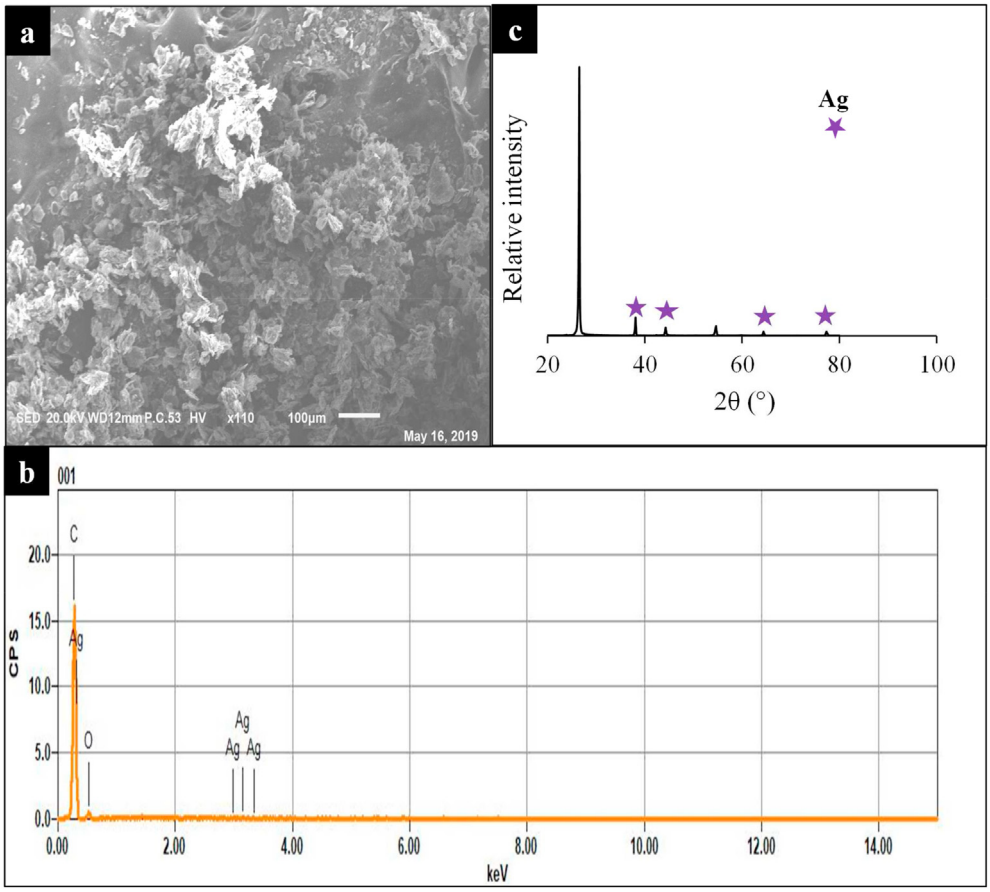

Figure 3. (a) SEM image of Ag@GrCE (b) EDS spectrum of Ag@GrCE (c) XRD spectrum of the Ag@GrCE.

suggest that some changes of the environment of silver particle deposited on the surface of graphite carbon. No new covalent bonding between the graphite carbon and Ag particles were formed. Which may be explained by silver particles immobilized and electron density of graphite carbon higher leading to weak O–H, C–H and C=C bands.

3.4. Electrocatalytic study of TXM reduction

3.4.1. Scan rate effect

The electrochemical mechanism of electrode process studied by the relationship between the peak current and potential scan rate. The scan rate effect on the reduction of 5.0×10^{-2} mol L^{-1} thiamethoxam at the silver particles deposited onto graphite electrode was investigated by cyclic voltammetry. With the increase of the scan rate, the reduction peak currents of TXM enhanced and peak potentials shifted to more negative values of potential. There is no reverse peak obtained for all the cyclic voltammetric scans, which shows that TXM undergo irreversible reduction on electrodeposited silver particles modified graphite electrodes (Figure 6a). The linear relationship between cathodic peak current of TXM (Ic) and scan rate (ν) plot is shown in the inset of Figure 6b, where the linear equation is $Ip = 0.0239 + 1.420\,\nu$, $R^2 = 0.966$. Moreover, a plot of the cathodic peak current versus the square root of scan rate ($\nu^{1/2}$)

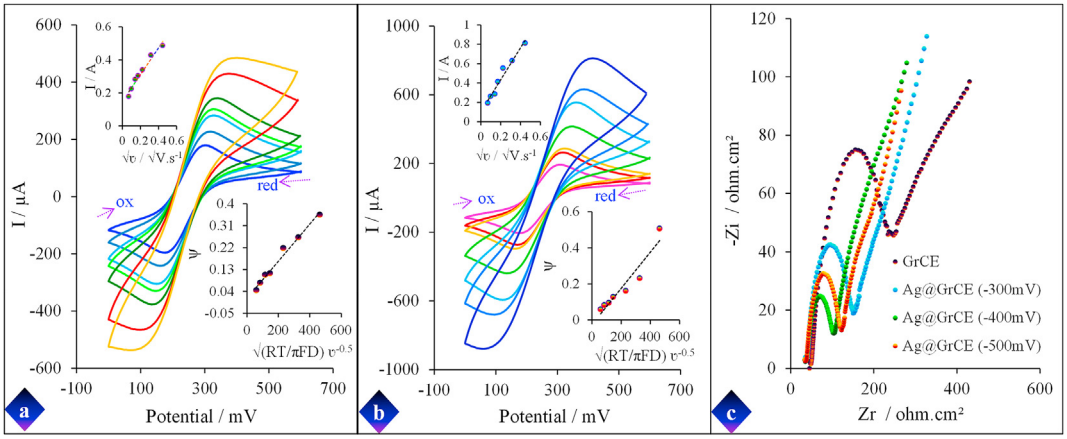

Figure 4. Cyclic voltammetry scan rate studies for $[Fe(CN)_6]^{3-/4-}$ at (a) GrCE and (b) Ag@GrCE Inset: ψ versus $[\pi DFn\nu/RT]^{-1/2}$; and Ip (µA) versus $\nu^{1/2}$. (c) The Nyquist diagrams of the impedance (Z_{im} vs. Z_{re}) for Ag@GrCE prepared at different applied potentials (-300 mV, -400 mV and -500 mV) and GrCE. Other conditions: 0.01 mol L^{-1} $K_3[Fe(CN)_6]$ and 0.1 mol L^{-1} KCl solutions.

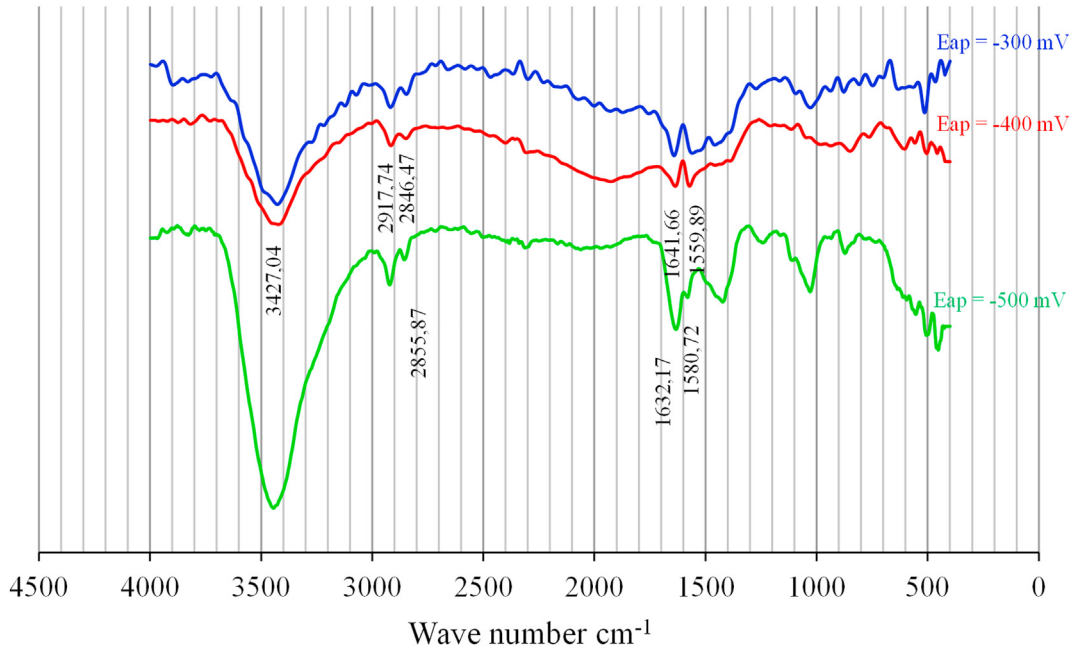

Figure 5. IR spectra of modified graphite carbon based on electrodeposited silver particles (Ag-GrC) prepared applying various potentials (-300, -400 and -500 mV).

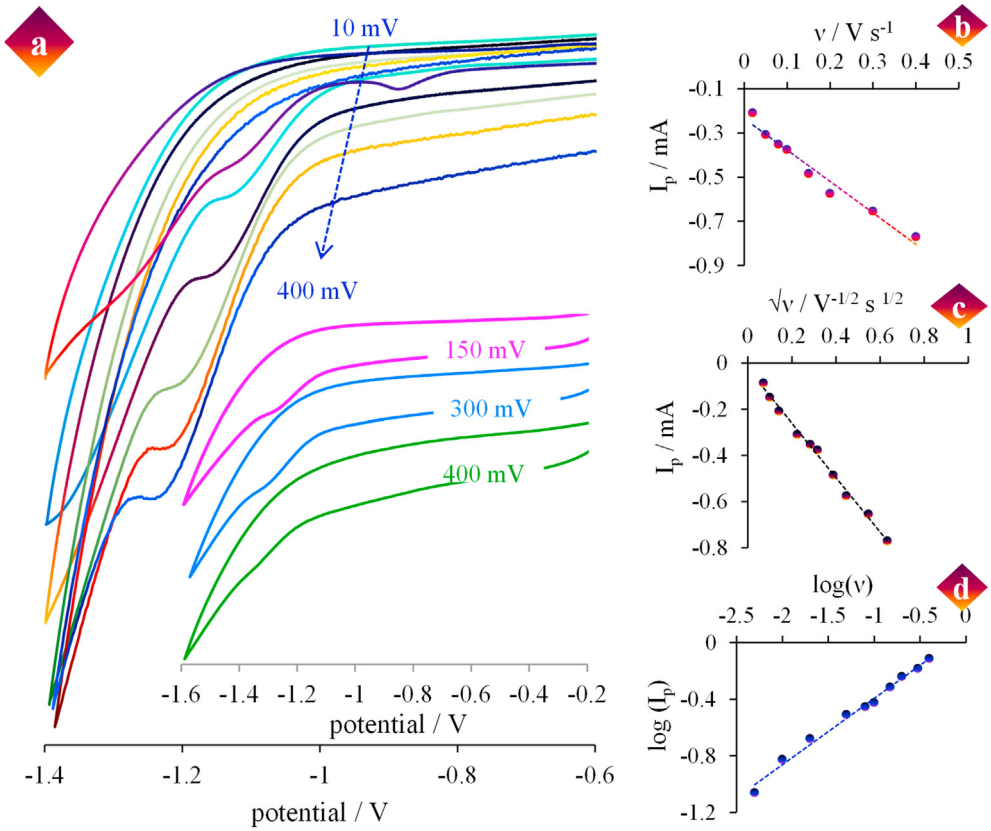

Figure 6. (a) Cyclic voltammograms recorded with carbon paste electrode modified electrodeposited silver particles in B-R buffer pH 10.4 containing 5.0×10^{-2} mol L^{-1} thiamethoxam at different scan rates. (b) The plot of cathodic peak current versus scan rate. (c) The Ic vs square root of scan rate. (d) The relationship between the logarithm of the peak currents versus the logarithm of scan rate.

yielded a straight line in the range of 10–400 mV s^{-1} (Figure 6c) according to the equation i_p (μA) = 0.0267 + 1.17 $\nu^{1/2}$ ($V^{1/2}$ $s^{1/2}$) (R^2 = 0.994). To confirm the TXM reduction control process, we rely on the slope value of linear plot between log (scan rate) and log (peak current) (Figure 6d). This slope value was found to be about 0.55, which very close to theoretical value (0.5) for the diffusion controlled reaction [60,

61]. Therefore, the result indicates that the electro-catalytic reduction of thiamethoxam at the Ag@GrCE was a typically diffusion-controlled electron transfer mechanism. As for an irreversible electrochemical reaction, the $E_{p,c}$ is determined by the following Eq. (5) [62].

$$Ep, c = E^{\circ} - \frac{RT}{\alpha nF}\ln(\frac{\alpha nF}{RTK}) - (\frac{RT}{\alpha nF})\ln(\upsilon) \quad (5)$$

E° is formal redox potential, k is the standard heterogeneous rate constant of electron transfer, n is electron transfer number involved in rate determining step, υ is scan rate, R is the gas constant, T is the absolute temperature, and F is the Faraday constant. According to the linear relationship of $E_{p,c}$ versus ln υ, the value of αn is defined according the slope (RT/αnF) of the fitted line to be -0.0353. Usually α is simulated to be between 0.3 to 0.7 in totally irreversible electrode process [63, 64, 65], then, the value of the electron transfer number n must to be around 3, and α is 0.3. The reduction of aromatic nitro compound R–NO_2 to hydroxylamine R–NHOH in aqueous media take place via four electrons. In alkaline medium, this reduction has been highlighted; essentially a 1e-reversible reduction is observed, followed by 3e-irreversible reduction [66, 67, 68]. In the present case, the studying peak correspond to second step three electrons and four-proton of nitro group TXM electro-reduction at Ag@GrCE in the alkaline media, because the 1e-reversible reduction of $RNO_2^{\cdot}$ is very small under these conditions, which can have illustrated as:

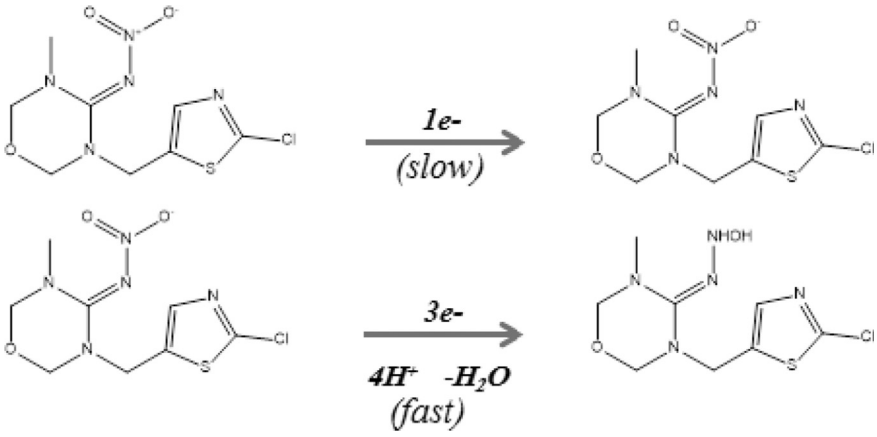

Consequently, the electrochemical mechanism consists of a mixture of diffusion and adsorption controlled processes depending on the scan rate [69, 70, 71, 72]. The adsorption capacity (Γ) for the reduction of thiamethoxam was determined to be 3.76 × 10^{-2} mol cm^{-2}, from the slope of the linear plot of I_p vs scan rate following Eq. (6):

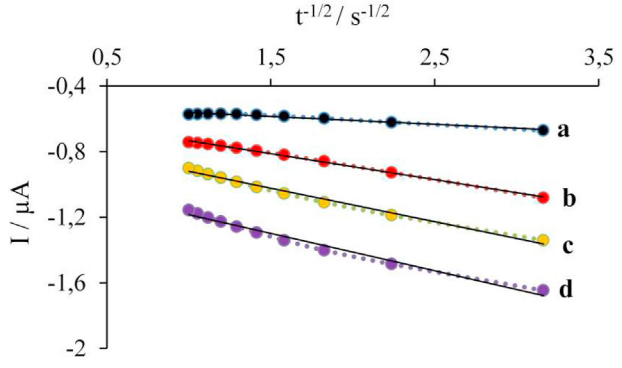

Figure 7. The plots of Ic vs. $t^{-1/2}$ ($s^{-1/2}$) obtained from chronoamperograms of thiamethoxam concentrations (a) 1.0 × 10^{-5}, (b) 2.5 × 10^{-5}, (c) 2.5 × 10^{-4} and (d) 1.0 × 10^{-3} mol L^{-1} with a potential step at −1100 mV in BR buffer (pH 10.4).

$$Ip = n^2F^2A\Gamma\nu/4RT \quad (6)$$

Where n is the number of electrons involved in the reaction; A is the geometric surface area of the electrode (0.1256 cm^2); v is scan rate; R, F and T have their normal meaning.

3.4.2. Chronoamperometric study

Chronoamperometric method was used to evaluate the catalytic performance of proposed electrode toward the electro reduction of thiamethoxam. The diffusion coefficient (D) was found to be about 1.55 × 10^{-2} cm^2 s^{-1} from the slope of the I_c vs $t^{-1/2}$ plot for different TXM concentrations (Figure 7) recorded at potential of -1100 mV, and employing the following Cottrell Eq. (7) [73]:

$$I = n.F.A.D^{1/2}.C.\pi^{-1/2}.t^{-1/2} \quad (7)$$

The rate constant of the electrocatalytic thiamethoxam reduction on Ag@GrCE was also determined using obtained chronoamperograms and the Galus Eq. (8) [74, 75, 76].

$$I_c/I_b = \pi^{1/2}\,(k.C.t)^{1/2} \quad (8)$$

Where C is the concentration of thiamethoxam in bulk solution, t is elapsed time, k is catalytic rate constant, I_b and I_C are the currents in the absence and presence of thiamethoxam, respectively. Therefore, Galus plots were made between I_c/I_b and $t^{1/2}$ for various concentrations, the mean value of the rate constant (k) was obtained to be about 1.67 × 10^4 mol L^{-1} s^{-1}.

3.5. Electro-analysis of thiamethoxam

3.5.1. Calibration graph and limit of detection

Square wave voltammetry was recorded under optimum instrumental setting: pulse 50 mV, amplitude modulation 10 mV, pH solution (10.4) and duration 1 mint. Square wave voltammetry responses of various concentrations of thiamethoxam in B-R buffer at Ag@GrCE are shown in Figure 8a. The cathodic peak current increased with increasing of TXM concentration ranging from 5.0 × 10^{-6} to 1.0 × 10^{-3} mol L^{-1}. The calibration plots illustrated good linear relationship between the peak current and the concentration of TXM (inset graph in Figure 8a). The linear regression is depicted by following equation. $I_c(\mu A)$ = 57647 [TXM] + 8.9179 with correlation coefficient of 0.9804. The limit of detection (LOD) and quantification (LOQ) were determined to be 1.92 × 10^{-6} and 6.34 × 10^{-6} mol L^{-1} respectively, calculated by equations LOD = 3×σ/s and LOQ = 10×σ/s where σ is the standard deviation of the blank and s is the slope of the calibration curve [77]. This value of detection limit is lower than that reported for a sensor based graphene oxide [78] and glassy carbon electrode [5].

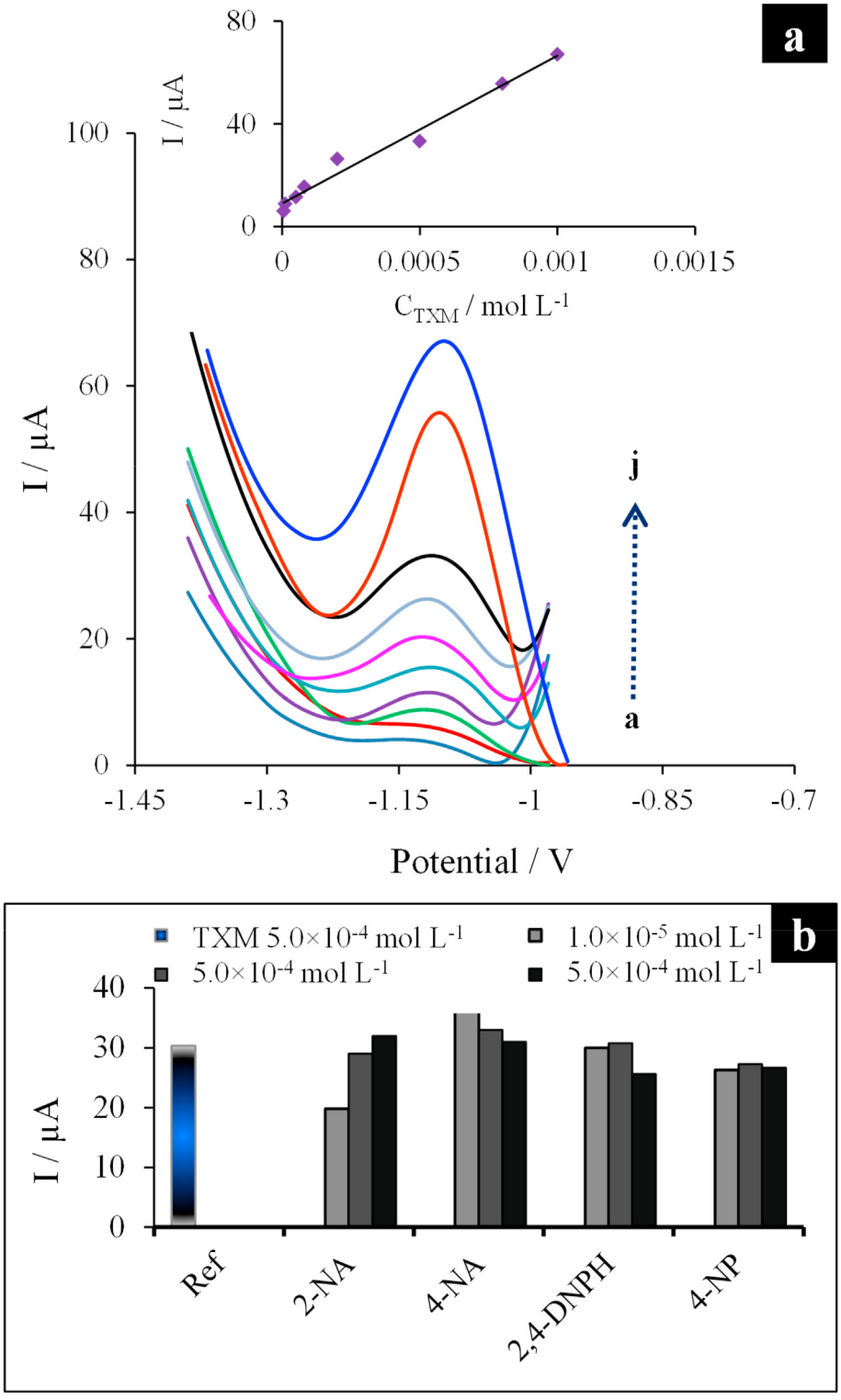

Figure 8. (a) Responses of square-wave voltammetry to increasing concentration of thiamethoxam (a: 5.0×10^{-6}, b: 8.0×10^{-6} c: 1.0×10^{-5}, d: 2.0×10^{-5}, e: 4.0×10^{-5}, f: 8.0×10^{-5}, g: 1.0×10^{-4}, h: 2.0×10^{-4}, i: 5.0×10^{-4}, j: 8.0×10^{-4} mol L^{-1}), with corresponding linear regression. All measurements were performed in Britton-Robinson buffer (pH 10.4) with electrodeposited Ag-particles modified GrCE. (b) Interferences study of different concentrations of nitro-organic species (1.0×10^{-5}, 1.0×10^{-4} and 5.0×10^{-4} mol L^{-1}) on the reduction signal of 5.0×10^{-4} mol L^{-1} thiamethoxam.

For evaluating the repeatability of this electrode, the TXM detection was performed 8 times repeatedly with an identical electrode. The relative standard deviations were 2.46 % and 4.37 % for 5.0×10^{-4} mol L^{-1} and 8.0×10^{-5} mol L^{-1}, respectively, showing a satisfactory repeatability of the Ag@GrCE. The storage stability of the modified electrode was also evaluated by measuring square wave voltammetry responses after storing the modified electrode for 2 weeks. The peak current slightly decreased of 10 % of the original response, showing an acceptable stability of the Ag@GrCE.

The selectivity of proposed electrode for the detection of thiamethoxam was examined in the presence of several nitro aromatics compounds (with different concentrations 1.0×10^{-5}, 1.0×10^{-4} and 5.0×10^{-4} mol L^{-1}) such as 4-nitrophenol (4-NP), 2-nitroaniline (2-NA), 4-nitroaniline (4-NA) and 2,4-dinitrophenylhydrazine (2,4-DNPH). Britton-robinson buffer solution (pH 10.4) containing 5.0×10^{-4} mol L^{-1} TXM was used (Figure 8b). The presence of these species did not show significant change in cathodic current intensity of TXM. The signal change observed was less than 5%, which indicates that organic species

Table 1. Recovery test of added samples. The study was done by spiking 1.0×10^{-4}, 5.0×10^{-4} and 1.0×10^{-3} mol L^{-1} of TXM in orange and tomato samples (n = 3 for each sample).

Sample	Added concentration [$\times 10^2$ µmol L^{-1}]	Found concentration [$\times 10^2$ µmol L^{-1}]	Recovery [%]	RSD, n = 3 [%]
Orange juice	10	9.7	97.001	1.025
	5	4.7	93.71	1.3
	1	0.9	90.17	3.3
Tomato juice	10	10.3	103.28	4.01
	5	4.37	92.07	0.91
	1	0.95	95.82	3.58

did not interfere the detection of TXM. Therefore, the proposed electrochemical sensor presents good selectivity toward TXM.

3.5.2. Practical samples determination

In order to evaluate its practical application, the electrodeposited silver particles on graphite electrode was employed to analyze TXM in orange and tomato juices samples. To do experiment, 25 mL of juice samples containing B-R buffer (pH 10.4) were tested. The concentration of TXM was found is lower than the LOD. So, both orange and tomato juices were contaminated with three knowing amounts of TXM. The recovery factor ranged from 95.82% to 103.28% for juice tomato sample and between 90.17% and 97.001% for juice orange sample with coefficients of variation lower than 4.01% (Table 1). These values belong the range 70–130% that fixed by the Environmental Protection Agency (EPA) [79]. From these measurements, it is obvious that developed electrode can be suitable for analysis of TXM in real samples.

4. Conclusion

In this paper, a novel electrochemical sensor has been developed, it is about an electrodeposited silver particles modified carbon electrode that has been manufactured and employed for the sensing of thiamethoxam. This electrode exhibits a great electrocatalytic activity toward thiamethoxam electro-reduction. Under the best experimental conditions, the square wave voltammetry method was used to determine the thiamethoxam with lower limit of detection in B-R buffer pH 10.4. The analytical utility of the proposed electrode was tested in real food samples (tomato an orange juices) with satisfactory results. Finally, the proposed method is thus opened new opportunities for detecting of neonicotinoids in food samples.

Declarations

Author contribution statement

Nourddine Ajermoun: Conceived and designed the experiments; Performed the experiments; Analyzed and interpreted the data; Wrote the paper.

Sara Lahrich, Sana Saqrane: Conceived and designed the experiments; Analyzed and interpreted the data.

Abdelfettah Farahi: Conceived and designed the experiments; Analyzed and interpreted the data; Wrote the paper.

Mina Bakasse: Analyzed and interpreted the data; Contributed reagents, materials, analysis tools or data.

Moulay Abderrahim El Mhammedi: Conceived and designed the experiments; Analyzed and interpreted the data; Contributed reagents, materials, analysis tools or data.

Funding statement

This research did not receive any specific grant from funding agencies in the public, commercial, or not-for-profit sectors.

Data availability statement

No data was used for the research described in the article.

Declaration of interests statement

The authors declare no conflict of interest.

Additional information

No additional information is available for this paper.

Acknowledgements

The authors would like to thank University Sultan Moulay Slimane of Beni Mellal, Morocco for supporting this work.

References

[1] P. Jeschke, R. Nauen, Neonicotinoids—from zero to hero in insecticide chemistry, Pest Manag. Sci. 64 (2008) 1084–1098.
[2] P. Jeschke, R. Nauen, M. Schindler, A. Elbert, Overview of the status and global strategy for neonicotinoids, J. Agric. Food Chem. 59 (2010) 2897–2908.
[3] M. Tomizawa, J.E. Casida, Neonicotinoid insecticide toxicology: mechanisms of selective action, Annu. Rev. Pharmacol. Toxicol. 45 (2005) 247–268.
[4] I. Yamamoto, J.E. Casida, Nicotinoid Insecticides and the Nicotinic Acetylcholine Receptor, Springer-Verlag, 1999.
[5] V.J. Guzsvany, F.F. Gaal, L.J. Bjelica, S.N. Okresz, Voltammetric determination of imidacloprid and thiamethoxam, J. Serb. Chem. Soc. 70 (2005) 735.
[6] A. Elbert, M. Haas, B. Springer, W. Thielert, R. Nauen, Applied aspects of neonicotinoid use in crop protection, Pest Manag. Sci. 64 (2008) 1099–1105.
[7] V. Guzsvány, M. Kádár, F. Gaál, K. Tóth, L. Bjelica, Rapid differential pulse polarographic determination of thiamethoxam in commercial formulations and some real samples, Microchim. Acta. 154 (2006) 321–328.
[8] Z.J. Papp, V.J. Guzsvany, S. Kubiak, A. Bobrowski, L. Bjelica, Voltammetric determination of the neonicotinoid insecticide thiamethoxam using a tricresyl phosphate-based carbon paste electrode, J. Serb. Chem. Soc. 75 (2010) 681–687.
[9] J.M. Bonmatin, C. Giorio, V. Girolami, D. Goulson, D.P. Kreutzweiser, C. Krupke, M. Liess, E. Long, M. Marzaro, E.A.D. Mitchell, N. Simon- Delso, A. Tapparo, D.A. Noome, Environmental fate and exposure; neonicotinoids and fipronil, Environ. Sci. Pollut. Res. 22 (2015) 35–67.
[10] H.C.J. Godfray, T. Blacquiere, L.M. Field, R.S. Hails, S.G. Potts, N.E. Raine, A.J. Vanbergen, A.R. McLean, A restatement of recent advances in the natural science evidence base concerning neonicotinoid insecticides and insect pollinators, Proc. R. Soc. B. 282 (2015) 1821.
[11] S. Kagabu, Chloronicotinyl insecticides-discovery, application and future perspective, Rev. Toxicol. 1 (1997) 75–129.
[12] P. Maienfisch, F. Brandl, W. Kobel, A. Rindlisbacher, R. Senn, CGA 293'343: a novel, broad-spectrum neonicotinoid insecticide, in: Nicotinoid Insecticides and the Nicotinic Acetylcholine Receptor, Springer, Tokyo, 1999, pp. 177–209.
[13] P. Maienfisch, H. Huerlimann, A. Rindlisbacher, L. Gsell, H. Dettwiler, J. Haettenschwiler, E. Sieger, M. Walti, The discovery of thiamethoxam: a second-generation neonicotinoid, Pest Manag. Sci. 57 (2001) 165–176.
[14] P. Maienfisch, M. Angst, F. Brandl, W. Fischer, D. Hofer, H. Kayser, W. Kobel, A. Rindlisbacher, R. senn, A. Steinemann, H. Widmer, Chemistry and biology of thiamethoxam: a second generation neonicotinoid, Pest Manag. Sci. 57 (2001) 906–913.
[15] N. Simon-Delso, V. Amaral-Rogers, L.P. Belzunces, J.M. Bonmatin, M. Chagnon, C. Downs, D. Goulson, Systemic insecticides (neonicotinoids and fipronil): trends, uses, mode of action and metabolites, Environ. Sci. Pollut. Res. (2015) 5–34.
[16] J. Ge, K. Cui, H. Yan, Y. Li, Y. Chai, X. Liu, J. Cheng, X. Yu, Uptake and translocation of imidacloprid, thiamethoxam and difenoconazole in rice plants, Environ. Pollut. 226 (2017) 479–485.

[17] S.R. Barik, P. Ganguly, S.K. Kunda, R.K. Kole, A. Bhattacharyya, Persistence behaviour of thiamethoxam and lambda cyhalothrin in transplanted paddy, Bull. Environ. Contam. Toxicol. 85 (2010) 419–422.

[18] X. Zhao, C. Wu, Y. Wang, T. Cang, L. Chen, R. Yu, Q. Wang, Assessment of toxicity risk of insecticides used in rice ecosystem on Trichogramma japonicum, an egg parasitoid of rice lepidopterans, J. Econ. Entomol. 105 (2012) 92–101.

[19] C. Anagnostopoulos, G.E. Miliadis, Development and validation of an easy multiresidue method for the determination of multiclass pesticide residues using GC–MS/MS and LC–MS/MS in olive oil and olives, Talanta 112 (2013) 1–10.

[20] Z. Xiao, Y. Yang, Y. Li, X. Fan, S. Ding, Determination of neonicotinoid insecticides residues in eels using subcritical water extraction and ultra-performance liquid chromatography–tandem mass spectrometry, Anal. Chim. Acta 777 (2013) 32–40.

[21] J.L. Vilchez, R. El-Khattabi, J. Fernández, A. González-Casado, A. Navalón, Determination of imidacloprid in water and soil samples by gas chromatography-mass spectrometry, J. Chromatogr., A 746 (1996) 289–294.

[22] Q. Fang, L. Wang, Q. Cheng, J. Cai, Y. Wang, M. Yang, X. Hua, F. Liu, A bare-eye based one-step signal amplified semiquantitative immunochromatographic assay for the detection of imidacloprid in Chinese cabbage samples, Anal. Chim. Acta 881 (2015) 82–89.

[23] H.J. Kim, S. Liu, Y.S. Keum, Q.X. Li, Development of an enzyme-linked immunosorbent assay for the insecticide thiamethoxam, J. Agric. Food Chem. 51 (2003) 1823–1830.

[24] J.K. Lee, K.C. Ahn, O.S. Park, S.Y. Kang, B.D. Hammock, Development of an ELISA for the detection of the residues of the insecticide imidacloprid in agricultural and environmental samples, J. Agric. Food Chem. 49 (2001) 2159–2167.

[25] E. Watanabe, K. Baba, H. Eun, S. Miyake, Application of a commercial immunoassay to the direct determination of insecticide imidacloprid in fruit juices, Food Chem. 102 (2007) 745–750.

[26] N. Ajermoun, A. Farahi, S. Lahrich, M. Bakasse, S. Saqrane, M.A. El Mhammedi, Electrocatalytic activity of the metallic silver electrode for thiamethoxam reduction: application for the detection of a neonicotinoid in tomato and orange samples, J. Sci. Food Agric. 99 (2019) 4407–4413.

[27] M. Putek, V. Guzsvány, B. Tasić, J. Zarębski, A. Bobrowski, Renewable silver-amalgam film electrode for rapid square-wave voltammetric determination of thiamethoxam insecticide in selected samples, Electroanalysis 24 (2012) 2258–2266.

[28] A. Kumaravel, M. Chandrasekaran, Nanosilver/surfactant modified glassy carbon electrode for the sensing of thiamethoxam, Sensor. Actuator. B Chem. 174 (2012) 380–388.

[29] V. Guzsvány, M. Kádár, F. Gaál, L. Bjelica, K. Tóth, Bismuth film electrode for the cathodic electrochemical determination of thiamethoxam, Electroynalysis (N.Y.N.Y.). 18 (2006) 1363–1371.

[30] A. Farahi, M. Achak, L. El Gaini, M.A. El Mhammedi, M. Bakasse, Electrochemical determination of paraquat in tomato at Ag/NP-modified graphite electrode using square wave voltammetry, Food Anal Methods 9 (2016) 139–147.

[31] M.A. El Mhammedi, M. Bakasse, R. Bachirat, A. Chtaini, Square wave voltammetry for analytical determination of paraquat at carbon paste electrode modified with fluoroapatite, Food Chem. 110 (2008) 1001–1006.

[32] Z. Papp, I. Švancara, V. Guzsvány, K. Vytřas, F. Gaál, Voltammetric determination of imidacloprid insecticide in selected samples using a carbon paste electrode, Microchim. Acta 166 (2009) 169–175.

[33] P. Chen, R.L. McCreery, Control of electron transfer kinetics at glassy carbon electrodes by specific surface modification, Anal. Chem. 68 (1996) 3958–3965.

[34] F. Laghrib, N. Ajermoun, M. Bakasse, S. Lahrich, M.A. El Mhammedi, Synthesis of silver nanoparticles assisted by chitosan and its application to catalyze the reduction of 4-nitroaniline, Int. J. Biol. Macromol. (2019).

[35] M.A. El Mhammedi, M. Achak, M. Bakasse, R. Bachirat, A. Chtaini, Accumulation and trace measurement of paraquat at kaolin-modified carbon paste electrode, Mater. Sci. Eng. C 30 (2010) 833–838.

[36] B. Rezaei, S. Damiri, Electrodeposited silver nanodendrites electrode with strongly enhanced electrocatalytic activity, Talanta 83 (2010) 197–204.

[37] E. Giannakopoulos, P. Stivaktakis, Y. Deligiannakis, Thermodynamics of adsorption of imidacloprid at constant charge hydrophobic surfaces: physicochemical aspects of bioenvironmental activity, Langmuir 24 (2008) 3955–3959.

[38] R.D.C.S. Luz, F.S. Damos, A.B. de Oliveira, J. Beck, L.T. Kubota, Voltammetric determination of 4-nitrophenol at a lithium tetracyanoethylenide (LiTCNE) modified glassy carbon electrode, Talanta 64 (2004) 935–942.

[39] Q. Shi, G. Diao, The electrocatalytical reduction of m-nitrophenol on palladium nanoparticles modified glassy carbon electrodes, Electrochim. Acta 58 (2011) 399–405.

[40] F. Laghrib, N. Ajermoun, A. Hrioua, S. Lahrich, A. Farahi, A. El Haimouti, M. Bakasse, M.A. El Mhammedi, Investigation of voltammetric behavior of 4-nitroaniline based on electrodeposition of silver particles onto graphite electrode, Ionics (2018) 1–9.

[41] M.R. Majidi, S. Ghaderi, Facile fabrication and characterization of silver nanodendrimers supported by graphene nanosheets: a sensor for sensitive electrochemical determination of Imidacloprid, J. Electroanal. Chem. 792 (2017) 46–53.

[42] F. Laghrib, M. Bakasse, S. Lahrich, M.A. El Mhammedi, Electrochemical sensors for improved detection of paraquat in food samples: a review, Mater. Sci. Eng. C (2019) 110349.

[43] P. Sebest, L. Fojt, V. Ostatna, M. Fojta, A. Danhel, Electrodeposited silver amalgam particles on pyrolytic graphite in (spectro) electrochemical detection of 4-nitro-phenol, DNA and green fluorescent protein, Bioelectrochemistry 132 (2020) 107436.

[44] F.H. Cho, S.C. Kuo, Y.H. Lai, Surface-plasmon-induced azo coupling reaction between nitro compounds on dendritic silver monitored by surface-enhanced Raman spectroscopy, RSC Adv. 7 (2017) 10259–10265.

[45] J. Bi, Electrodeposited silver nanoflowers as sensitive surface-enhanced Raman scattering sensing substrates, Mater. Lett. 236 (2019) 398–402.

[46] J. Klug, M.F. Torresan, F. Lurgo, G. Borioli, G.I. Lacconi, A spectroscopic sensing platform for MARCKS protein monolayers, J. Colloid Interface Sci. 508 (2017) 532–541.

[47] M. Baghayeri, M.B. Tehrani, A. Amiri, B. Maleki, S. Farhadi, A novel way for detection of antiparkinsonism drug entacapone via electrodeposition of silver nanoparticles/functionalized multi-walled carbon nanotubes as an amperometric sensor, Mater. Sci. Eng. C 66 (2016) 77–83.

[48] H. Zhai, Z. Liang, Z. Chen, H. Wang, Z. Liu, Z. Su, Q. Zhou, Simultaneous detection of metronidazole and chloramphenicol by differential pulse stripping voltammetry using a silver nanoparticles/sulfonate functionalized graphene modified glassy carbon electrode, Electrochim. Acta 171 (2015) 105–113.

[49] L.A. Goulart, R. Gonçalves, A.A. Correa, E.C. Pereira, L.H. Mascaro, Synergic effect of silver nanoparticles and carbon nanotubes on the simultaneous voltammetric determination of hydroquinone, catechol, bisphenol A and phenol, Microchim. Acta. 185 (2018) 12.

[50] M. Roushani, F. Shahdost-fard, A glassy carbon electrode with electrodeposited silver nanoparticles for aptamer based voltammetric determination of trinitrotoluene using riboflavin as a redox probe, Microchim. Acta. 185 (2018) 558.

[51] J. Tang, Y. Huang, C. Zhang, H. Liu, D. Tang, DNA-based electrochemical determination of mercury (II) by exploiting the catalytic formation of gold amalgam and of silver nanoparticles, Microchim. Acta 183 (2016) 1805–1812.

[52] A. Tiwari, T.C. Nagaiah, Dioxygen reduction by nitrogen-rich mesoporous carbon bearing electrodeposited silver particles, ChemCatChem 8 (2016) 396–403.

[53] A. Wang, Y.F. Huang, U.K. Sur, D.Y. Wu, B. Ren, S. Rondinini, C. Amatore, Z.Q. Tian, In situ identification of intermediates of benzyl chloride reduction at a silver electrode by SERS coupled with DFT calculations, J. Am. Chem. Soc. 132 (2010) 9534–9536.

[54] A. Kumaravel, M. Chandrasekaran, A novel nanosilver/nafion composite electrode for electrochemical sensing of methyl parathion and parathion, J. Electroanal. Chem. 638 (2010) 231–235.

[55] G. Mitrikas, Y. Deligiannakis, C.C. Trapalis, N. Boukos, G. Kordas, CW and pulsed EPR study of silver nanoparticles in a SiO2 matrix, J. Sol. Gel Sci. Technol. 13 (1998) 503–508.

[56] P.A. Swarthmore, Joint Committee on Powder Diffraction Standards Diffraction Data File, JCPDS International Center for Diffraction Data, 1991.

[57] R.S. Nicholson, Theory and application of cyclic voltammetry for measurement of electrode reaction kinetics, Anal. Chem. 37 (1965) 1351–1355.

[58] I. Lavagnini, R. Antiochia, F. Magno, An extended method for the practical evaluation of the standard rate constant from cyclic voltammetric data, Electroynalysis (N.Y.N.Y.). 16 (2004) 505–506.

[59] R.J. Klingler, J.K. Kochi, Electron-transfer kinetics from cyclic voltammetry. Quantitative description of electrochemical reversibility, J. Phys. Chem. 85 (1981) 1731–1741.

[60] E. Laviron, L. Roullier, C. Degrand, A multilayer model for the study of space distributed redox modified electrodes: Part II. Theory and application of linear potential sweep voltammetry for a simple reaction, J. Electroanal. Chem. Interfacial Electrochem. 112 (1980) 11–23.

[61] Y. Zhou, W. Tang, J. Wang, G. Zhang, S. Chai, L. Zhang, T. Liu, Selective determination of dopamine and uric acid using electrochemical sensor based on poly (alizarin yellow R) film-modified electrode, Anal. Methods 6 (2014) 3474–3481.

[62] E. Laviron, Adsorption, autoinhibition and autocatalysis in polarography and in linear potential sweep voltammetry, J. Electroanal. Chem. Interfacial Electrochem. 52 (1974) 355–393.

[63] A.J. Bard, L.R. Faulkner, J. Leddy, C.G. Zoski, Electrochemical Methods: Fundamentals and Applications, 2, wiley, New York, 1980.

[64] S.Q. Liu, H.X. Ju, Renewable reagentless hydrogen peroxide sensor based on direct electron transfer of horseradish peroxidase immobilized on colloidal gold-modified electrode, Anal. Biochem. 307 (2002) 110–116.

[65] S. Liu, Z. Dai, H. Chen, H. Ju, Immobilization of hemoglobin on zirconium dioxide nanoparticles for preparation of a novel hydrogen peroxide biosensor, Biosens. Bioelectron. 19 (2004) 963–969.

[66] E. Laviron, A. Vallat, R. Meunier-Prest, The reduction mechanism of aromatic nitro compounds in aqueous medium: Part V. The reduction of nitrosobenzene between pH 0.4 and 13, J. Electroanal. Chem. 379 (1994) 427–435.

[67] R. Lacasse, R. Meunier-Prest, E. Laviron, A. Vallat, The reduction mechanism of aromatic nitro compounds in aqueous medium Part 3. The reduction of 4-nitro-pyridine-N-oxide between H0=− 6 and pH 9, J. Electroanal. Chem. 359 (1993) 223–239.

[68] E. Laviron, R. Meunier-Prest, R. Lacasse, The reduction mechanism of aromatic nitro compounds in aqueous medium. Part IV. The reduction of p-nitrobenzophenone between H0=− 5 and pH 14, J. Electroanal. Chem. 375 (1994) 263–274.

[69] M.P. Siswana, K.I. Ozoemena, T. Nyokong, Electrocatalysis of asulam on cobalt phthalocyanine modified multi-walled carbon nanotubes immobilized on a basal plane pyrolytic graphite electrode, Electrochim. Acta 52 (2006) 114–122.

[70] A. Salimi, C.E. Banks, R.G. Compton, Abrasive immobilization of carbon nanotubes on a basal plane pyrolytic graphite electrode: application to the detection of epinephrine, Analyst 129 (2004) 225–228.

[71] A. Salimi, L. Miranzadeh, R. Hallaj, Amperometric and voltammetric detection of hydrazine using glassy carbon electrodes modified with carbon nanotubes and catechol derivatives, Talanta 75 (2008) 147–156.

[72] J.S. Ye, Y. Wen, W. De Zhang, H.F. Cui, Q.G. Xu, F.S. Sheu, Electrochemical biosensing platforms using phthalocyanine-functionalized carbon nanotube electrode, Electroynalysis (N.Y.N.Y.). 17 (2005) 89–96.
[73] M.A. Prathap, V. Anuraj, B. Satpati, R. Srivastava, Facile preparation of Ni (OH) 2–MnO_2 hybrid material and its application in the electrocatalytic oxidation of hydrazine, J. Hazard Mater. 262 (2013) 766–774.
[74] G.C. Barker, E. Galus, Fundamentals of Electrochemical Analysis, Ellis Horwood Ltd., Chichester, 1976, pp. 182–183, 520+ xviii pp.,£ 23.50" (1977).
[75] N. Rastakhiz, H. Beitollahi, A. Kariminik, F. Karimi, Voltammetric determination of carbidopa in the presence of uric acid and folic acid using a modified carbon nanotube paste electrode, J. Mol. Liq. 172 (2012) 66–70.
[76] S. Kavian, S.N. Azizi, S. Ghasemi, Electrocatalytic detection of hydrazine on synthesized nanozeolite-supported Ag nanoparticle-modified carbon paste electrode at a negative potential in an alkaline medium, J. Mol. Liq. 218 (2016) 663–669.
[77] D. Skoog, J. Holler, T. Nieman, Principles of Instrumental Analysis, fifth ed., Harrcourt Brace College Publishers, Orlando Florida, 1998, pp. 13–14.
[78] V. Urbanová, A. Bakandritsos, P. Jakubec, T. Szambó, R. Zbořil, A facile graphene oxide based sensor for electrochemical detection of neonicotinoids, Biosens. Bioelectron. 89 (2017) 532–537.
[79] S.A. Paula, O.A.E. Ferreira, P.A. César, Determination of imidacloprid based on the development of a glassy carbon electrode modified with reduced graphene oxide and manganese (ii) phthalocyanine, Electroanalysis 32 (2020) 86–94.